Transition from wave- to tide-dominated estuary: An example from the Eocene Urahoro Group, eastern Hokkaido, northern Japan

Ryusei Sato[a,*], Hajime Naruse[a]

[a]Department of Geology and Mineralogy, Graduate School of Science, Kyoto University,

Kitashirakawaoiwake-cho, Sakyo-ku, Kyoto 606-8502, Japan

* Corresponding author E-mail: sato.ryusei.44e@st.kyoto-u.ac.jp (R. Sato).

ABSTRACT

Estuarine morphologies are commonly classified into two end-member categories based on dominant sediment transport processes: wave-dominated and tide-dominated estuaries. Although estuaries are generally presumed to retain their fundamental morphotypes throughout their evolutionary history, this study presents the first documented ancient example of a morphological transition from a wave-dominated to a tide-dominated estuary, identified in the Eocene Urahoro Group in eastern Hokkaido, Japan. A three-dimensional outcrop model was utilized to generate continuous stratigraphic columns extending into the upper parts of the outcrop for detailed facies analysis. Seven facies were identified and grouped into three stratigraphically successive facies associations: (1) an alluvial fan association characterized by braided river channels and floodplain deposits; (2) a wave-dominated estuary association comprising the bayhead delta, central basin, and flood-tidal delta deposits; and (3) a tide-dominated estuary association consisting of tidal sand bar and tidal flat deposits. This study proposes a hypothesis to explain this unusual evolutionary transition: an accelerated relative sea-level rise likely enhanced tidal influences, causing barrier disintegration within the initially wave-dominated estuarine system. These findings emphasize the potential for more dramatic morphological changes in estuarine systems than previously recognized, providing critical insights into predicting estuarine responses to future environmental changes.

Keywords: coastal morphodynamics, facies analysis, sea-level rise, barrier disintegration, three-dimensional outcrop model

1 INTRODUCTION

Estuaries are coastal depositional systems that typically develop in drowned incised valleys infilled with fluvial to marine sediments (Dalrymple et al., 1992; Allen and Posamentier, 1993; Boyd et al., 2006). The diversity of estuary architectures has been attributed to variations in the environmental factors influencing the systems (Roy et al., 1980; Chaumillon et al., 2010). These environmental factors include sea-level changes, grain-size distribution, and sediment transport by rivers, tides, and waves, and some of them are interrelated with each other (Allen, 1971; Roy et al., 1980; Dalrymple et al., 1992; Cooper, 1993; Dissanayake et al., 2012; Khojasteh et al., 2021). Among these, waves and tidal activities are the fundamental conditions determining the morphological types of estuaries.

Thus, the two end-member classification of estuaries was established by Dalrymple et al. (1992) based on the dominant sediment transport processes: wave-dominated and tide-dominated estuaries. A wave-dominated estuary is an estuary where barrier architecture, central basins, and bayhead delta develop (Roy et al., 1980; Dalrymple et al., 1992). On the other hand, the tide-dominated estuary is characterized by tidal sand bars, extensive tidal flats, and a tidal-fluvial channel (Dalrymple et al., 1990; Dalrymple and Choi, 2007).

Estuaries are expected to maintain their morphological types throughout their evolutionary histories. Estuarine development paths vary depending on the balance of sediment supply between river and marine environments, in addition to the rate of sea-level changes. Several evolutionary models for estuaries have been proposed based on observations of Holocene transgression to highstand stages. Some wave-dominated estuaries eventually become deltas because of the infilling of the back-barrier regions are infilled by fluvial systems without changing their wave-dominated characteristics (Roy et al., 1980; Dalrymple et al., 1992; Harris and Heap, 2003). However, other wave-dominated estuaries can transit from transgressive to regressive systems to sustain mouth barriers when the fluvial sediment supply is insufficient (Roy et al., 1980; Anthony et al., 2002). On the other hand, tide-dominated estuaries are also expected to maintain their characteristic funnel-shaped shorelines and finally shift to deltas (Harris and Heap, 2003). These evolutionary models consistently suggest that essential estuarine morphologies do not change temporally until they develop into deltas.

Unlike the conventional view, however, tide-dominated estuaries can temporally change their morphological features under specific conditions. Pendón et al. (1998) and Williams et al. (2013) documented the Holocene estuarine transitions from tide- to wave-dominated morphologies in southwestern Spain and southeastern South Korea, respectively. These estuaries have experienced morphological transitions in response to changes in environmental factors, such as the development of adjacent coastal systems and anthropogenic alterations. These examples suggest that tide-dominated estuaries can drastically change their morphologies because of changes in environmental factors, which may even modify the dominant sediment transport mechanism.

Nevertheless, evolutionary models addressing morphological transitions in wave-dominated estuaries are rare. Although wave-dominated estuaries are generally expected to maintain their fundamental morphologies until they develop into deltas, recent observations indicate that significant morphological changes are occurring in modern wave-dominated environments. Sea-level changes play a key role in the long-term evolution of barrier systems. Due to the recent acceleration of sea-level rise, coastal barrier disintegration has been observed globally (Moore et al., 2010; Lorenzo-Trueba and Ashton, 2014; FitzGerald et al., 2018). In conjunction with rising sea levels, storms have become more frequent and intense, significantly contributing to erosional processes that affect barrier system morphodynamics (Zhang et al., 2002; Masselink and van Heteren, 2014; Kumbier et al., 2018). To predict the future evolution of wave-dominated estuaries, it is essential to understand how estuarine morphologies can respond to changes in environmental factors.

In this paper, we investigate the Eocene Urahoro Group in eastern Hokkaido, Japan, as an exceptional ancient example of a transition from a wave-dominated to a tide-dominated estuary. Well-exposed estuarine deposits along coastal cliffs provide continuous transitional successions, allowing for a comprehensive spatial understanding of facies distribution. To complement field observations, we employed three-dimensional (3D) outcrop models generated through drone-based photogrammetry to enhance the characterization of estuarine facies. Seven facies were identified and classified into three facies associations in ascending stratigraphic order: alluvial fan, wave-dominated estuary, and tide-dominated estuary. Possible mechanisms driving the transition from a wave- to tide-dominated estuary are discussed, considering sea level changes. This research advances the understanding of estuarine morphodynamics based on ancient deposits, offering valuable insights for predicting future estuarine evolution.

2 GEOLOGICAL SETTINGS

The Eocene Urahoro Group is 400–1000 m thick deposits composed of fluvial to shallow marine facies (Sasa, 1940a,b). The Urahoro Group is distributed in eastern Hokkaido, northern Japan (Fig.1A). The group is distributed along the subduction zone of the Pacific Plate and is considered to comprise part of the Paleo-Kuril Arc, which collided with the North-Eastern Japan Arc in the Paleogene. According to paleomagnetic analysis, Katagiri et al. (2020) revealed that the Urahoro Group was deposited during the arc-arc collision of the two magmatic island arcs.

This group is exposed in two separated regions (Fig.1B). The western region of distribution is the Shiranuka Hill region, and the eastern part is the Konsen Coastal region in eastern Hokkaido, northern Japan. In the Konsen Coastal Region, beds in the Urahoro Group dip gently (mostly less than 10°) into various directions, indicating a weakly folded structure (Nanayama et al., 1994; Nagahama, 1961). On the other hand, in the Shiranuka Hill region, the Urahoro Group is characterized by intense tectonic folds and faults due to terrane deformation and rotation during arc-arc collision (Katagiri et al., 2020). The Group unconformably overlays the Upper Cretaceous to Paleogene Nemuro Group. In the Shi- ranuka Hill region, the Urahoro Group is unconformably overlain by the Lower Oligocene Onbetsu Group (Matsui, 1962).

The Urahoro Group was mainly deposited around 40 Ma, which corresponds to the Bartonian, the upper Eocene. The Urahoro Group in the Konsen Coastal region is composed of six formations: the Beppo, Harutori, Tenneru, Yubetsu, Shitakara, and Shakubetsu Formations in ascending stratigraphic order (Sasa, 1940a and Sasa, 1940b). The Rushin Formation is only exposed in the Shiranuka Hill region, and it can be correlated to the lower three Formations (the Beppo, Harutori, and Tenneru Formations) in the Konsen Coastal region (Tanai, 1957). The depositional age of the Group is estimated to be approximately 40 Ma according to Zircon U-Pb radiometric dating of the Harutori and Tenneru Formations (Katagiri et al., 2016, 2020). Paleomagnetic analysis indicated that the Yubetsu and Rushin Formations were deposited in the polarity chron 18.1n, which ranges from 39.6 to 38.6 Ma (Katagiri et al., 2020; Ogg, 2012).

This study investigated the facies and depositional environments of the Tenneru, Yubetsu, and Shitakara Formations exposed in the Konsen Coastal region (Figs.1C and 3). The Tenneru Formation is primarily composed of conglomerates interbedded with thin sandstones and coaly mudstones. The Yubetsu Formation is subdivided into two members: the Yubetsu and Shimizu members (Kawai, 1956). The Yubetsu member is the lower part of the Yubetsu Formation and consists of alternating beds of coaly mudstone and sandstone intercalating conglomerates (Kawai, 1956). The Shimizu member is the upper part of the Formation, which is composed of thick mudstone intercalating with sandy mudstone and fine sandstone layers and yields *Corbicula* sp. (Kawai, 1956). The Shitakara Formation is mainly composed of sandstone interbedded with granule conglomerates. This Formation abundantly yields molluscan fossils including *Ostrea* sp. and *Nemocardium* sp., and is supposed to show brackish and marine facies (Matsui, 1962).

Paleocurrent analysis and gravel composition suggested that the sediment source of these formations was located in the western region where the accretionary complex exposed (Sato et al., 1967). On the other hand, conglomerates of the Beppo and Harutori Formations below the surveyed formations were supplied from the eastern region. This sediment provenance transition is attributed to the uplift of the Upper Cretaceous to Paleogene Nikoro Group, which is an accretionary complex of the Paleo-Kuril Arc (Sato et al., 1967; Nanayama et al., 1994). Because of the change in sediment provenance, the conglomerates of the Beppo and Harutori Formations are composed of black gravels of igneous rocks (Nanayama et al., 1994; Nagahama, 1961). In contrast, the conglomerates of the Tenneru, Yubetsu, and Shitakara Formations are characterized by red chart gravels (Nanayama et al., 1994).

3 FACIES ANALYSIS

For the facies analysis, a drone was utilized to investigate the sedimentary deposits exposed on outcrops that researchers could not reach. This study surveyed the Urahoro Group in the Konsen Coastal Region because of its good exposure along the coastal cliffs. To generate columnar sections continuously to the upper part of the outcrop, a drone was leveraged to take outcrop photographs, which were also used to construct a 3D outcrop model using the photogrammetry method. The 3D outcrop model enabled us to understand the geological architecture of the sedimentary deposits on a large-scale outcrop and observe them in the laboratory.

Seven facies were identified based on bed geometry, grain size, sedimentary structures, and fossils (Fig.2), which comprise three facies associations: alluvial fan, wave-dominated, and tide-dominated estuaries (Fig.3).

3.1 Facies Association I: Alluvial fan

3.1.1 Facies 1: braided river channel

Description. Facies 1 is mainly composed of poorly sorted sandstones and clast-supported conglomerates consisting mainly of angular to subangular red chart gravels. The grain size of the conglomerates ranges from granule to cobble. Beds exhibit upward fining trends and vary significantly in thickness, from 0.1 m to 3 m, comprising bed sets with more than 10 m in the maximum thickness (Fig.4A). The bounding erosional surfaces of the bed sets are planar to concave-upward in geometry (Fig.4A). The trough cross-stratification is well-developed in this facies (Fig.4C). The paleocurrents measured in the Mitsuura and Poronai regions were mainly eastward (Fig.4B).

Interpretation. Facies 1 exhibits typical features of channel deposits of braided rivers. It is known that the channel deposits of braided rivers are composed of channel-bar and channel-fill deposits, both of which exhibit multiple fining-upward beds with unidirectional cross-stratification (Bridge, 2006). Channel-fill deposits are distinguished by concave-upward erosional bases, while the bar deposits are accompanied by planar bounding surfaces (Allen, 1983; Bridge, 2006; Bridge and Lunt, 2006; Sambrook Smith et al., 2006). These features are common in Facies 1 (Figs.4A and C). The grain size of the granule to cobble in Facies 1 infers gravel bedload connected to the active uplift areas (Miall, 2010; Nichols and Fisher, 2007).

3.1.2 Facies 2: floodplain

Description. Facies 2 consists of alternations of sandstones and mudstones. The thickness of each bed ranges from 10 cm to 1 m and exhibits lateral-thinning trends (Fig.4D). The sandstones are muddy, fine-grained, and sometimes weakly laminated. The mudstones are massive and commonly contain small wood fragments. The sandstones and mudstones of Facies 2 often include rootlet fossils and are interbedded with coal seams less than 20 cm thick. Facies 2 is intercalated within the conglomerates of Facies 1 and is bounded by irregular erosional surfaces.

Interpretation. Facies 2 is interpreted as a floodplain deposit. These deposits are characterized by fine-grained sandstone intercalated with mudstone layers that originated from overflowing floods or flows from crevasse channels (Bridge, 2006). The presence of rootlet fossils and coal seams is typical of floodplain environments (Miall, 1981). The lateral thinning trend is attributed to the increased distance from active channels (Bridge, 2003; Bridge, 2006). The superimposition of Facies 1 and 2 likely reflects channel migration and avulsion processes within the braided river system.

3.1.3 Depositional Environment of Facies Association I

Alluvial fan facies association is composed of the deposits of the braided river channel (Facies 1) and the floodplain (Facies 2). This facies association occurs at the lowermost part of the Urahoro Group in the study area (Fig.3). According to the paleocurrents measured from Facies 1, the sediment source of this facies association is interpreted to have been located on the west side of the depositional basin (Fig.4B).

3.2 Facies Association II: Wave-dominated estuary

3.2.1 Facies 3: bayhead delta

Description. Facies 3 consists of medium to coarse sandstones containing granules and pebbles intercalated in coaly mudstones. The gravels are mainly composed of moderately sorted angular or subangular red charts. The composition of the conglomerates is similar to that of Facies 1, whereas the grain size is finer and more sorted in Facies 3. The sandstones are cross-stratified and have erosional bases (Fig.5A). The paleocurrents are mainly toward the east (Fig.6A), and they do not contradict those in the fluvial deposits of Facies 1. Rootlet fossils are included in the sandstones and mudstones. This facies occasionally interbeds fine-grained sandstones exhibiting wave ripples and mud drapes(Fig.5B).

Interpretation. Facies 3 is interpreted as bayhead delta deposits. Bayhead deltas are small-scale deltas located in the landward part of estuaries, where the freshwater enters the brackish environment (Aschoff et al., 2018). The rootlet fossils indicate that the cross-stratified sandstones and coaly mudstones are channel-fill and floodplain deposits in the top set of the bayhead delta. The sandstones with wave ripples and mud drapes indicate the influence of tides and waves that rework sediment in a shallow marine environment (Reineck and Wunderlich, 1968; Aschoff et al., 2018), corresponding to the foreset of the bayhead delta. The wave and tidal influences in Facies 3 discriminate this facies from alluvial fan deposits (Boyd et al., 2006). The abundance of organic matters is typical in bayhead deltas (Anthony et al., 2002). The interposition of the fluvial (topset) and foreset deposits implies temporal and spatial fluctuations in the ratio between relative sea-level rise and fluvial sediment input (Aschoff et al., 2018; Simms et al., 2018).

3.2.2 Facies 4: central basin

Description. Facies 4 is composed of laminated mudstones with intercalations of very thin-bedded fine sandstone laminae, which abundantly yield *Corbicula* sp. and small wood fragments (Figs.5C and 6A). Discontinuous sand lenses of a few millimeters in thickness are ubiquitous, and bioturbation is nearly absent. Medium-grained parallel and wave-ripple laminated sandstones are observed at the boundary between the coaly mudstones of Facies 3 and this facies (Fig.5A and 6A).

Interpretation. Facies 4 is interpreted as central basin deposits. A central basin constitutes the low-energy central part of the wave-dominated estuary, acting as the prodelta region of the bayhead delta (Dalrymple et al., 1992). Abundant occurrences of *Corbicula* sp. are typical in brackish water environments (Meijer and Preece, 2000). The intercalated sandstone laminae are deposits of episodic events such as storms or floods (Nichols et al., 1991). The parallel and wave-ripple laminated sandstone bed at the base of this facies can be interpreted as marginal tidal flat deposits.

3.2.3 Facies 5: flood tidal delta

Description. Facies 5 consists of fine- to medium-grained muddy sandstones, comprising the uppermost part of Facies Association II (Fig.6A). The thickness of this facies is ~10 m. The sandstone is characterized by abundant wavy-flaser ripples (Fig.7A). *Nemocardium* sp. and *Ostrea* sp. are often observed. This facies exhibits an upward-fining trend and is sometimes parallel-stratified with nodular beds. The lower part of this facies is mainly composed of poorly sorted medium-to-coarse sandstones with sub-rounded pebbles and molluscan fossils, overlying the mudstone of Facies 4 (Fig.6A and 5D). The bounding surface with Facies 4 is intensely bioturbated by *Gyrolithes* isp. and is characterized by burrows of a few cm in diameter with branching and spiral shapes (Fig.5E). These burrows were filled with coarse-grained sandstones that penetrated the underlying mudstones of Facies 4.

Interpretation. Facies 5 is interpreted as flood-tidal delta deposits near the estuarine mouth barrier. Flood-tidal delta deposits are generally bioturbated sandy deposits transported landward through tidal inlets at mouth barriers (Hayes and FitzGerald, 2013). The occurrence of coarse-grained deposits and shell fragments underlying central basin mudstones (Facies 4) is a typical feature of deposition in flood-tidal deltas (Nichols et al., 1991; Dalrymple et al., 1992). *Nemocardium* sp. and *Ostrea* sp. are marine and brackish species (Wells, 1961), respectively, indicating that Facies 5 was possibly deposited in a brackish environment receiving sediment supply from the marine environment. *Gyrolithes* isp is an indicator of brackish environments, particularly of estuaries (Boyd et al., 2006), and it further suggests a transitional environment between freshwater and marine water, such as an estuary mouth (de Fátima Rossetti, 2000). Wavy-flaser ripples are bedform influenced by tide and wave (Reineck and Wunderlich, 1968), suggesting intertidal shoals and sand flat deposits (Nio et al., 1980; Richards, 1994).

3.2.4 Depositional Environment of Facies Association II

Facies Association II is interpreted as a wave-dominated estuary deposit, which consists of deposits of the bayhead delta (Facies 3), the central basin (Facies 4), and the flood-tidal delta (Facies 5) (Fig.6B). This facies association gradually overlies Facies Association I, which is identified by the grain-size fining of conglomerates (Fig.3). The paleocurrent directions observed in the fluvial channel deposits (Facies 1) and the bayhead delta deposits (Facies 3) are oriented mainly toward the east (Figs.4B and 6A), indicating that the terrestrial sediment source was located on the west side of the depositional basin. As discussed later, this wave-dominated estuarine system (Facies Association II) changed to a tide-dominated estuarine system (Facies Association III) at the top. The barrier system that blocked the mouth of the wave-dominated estuary would have been disintegrated and reworked by the tidal currents at this transition. The thick sandy near-estuarine mouth deposits (Facies 5) that develop at the top of Facies Association II may be the result of this reworking of the barrier.

3.3 Facies association III: Tide-dominated estuary

This facies association is superbly exposed in the coastal cliff along the Konbumori coast (Fig.1C) where the Urahoro Group crops out 400 m wide and ~50 m high. The constructed 3D outcrop model was used for facies observations (Fig.8A).

3.3.1 Facies 6: tidal sand bar

Description. Facies 6 is mainly composed of medium- to coarse-grained sandstone, occasionally interbedded with granule stratification. The coarse sandstone and granules primarily comprise red charts, as in Facies 1 and 3. This facies is marked by trough cross-stratification exhibiting multidirectional paleocurrents (Fig.6A). The cross-stratified sandstones often pinch out laterally because of their overlying erosional surfaces (Fig.8B). The set heights of the cross-stratification are divided into two scales: large- (1–2 m) (Fig.7C and 8D) and small-scales (10–20 cm) (Figs.7D and 8D). Mud drapes are common in small-scale cross- stratification (Fig.7D). Double mud drapes (paired mud drapes) can be seen (Fig.7E). At the lowermost boundary of Facies 6, a pebble conglomerate abundantly yielding *Ostrea* sp. (Figs.7A and B) occurs. The gravels included in this facies are well-sorted and rounded to subrounded.

Interpretation. Facies 6 is interpreted as tidal sand bar deposits. Tidal sand bars are elongated sand bodies formed by complex tidal channel networks in tide-dominated coasts (Dalrymple and Choi, 2007). Tidal sand bar deposits are identified by cross-stratified medium- to coarse-grained sandstones with multidirectional paleocurrents due to landward and seaward sediment transport by flood and ebb currents, respectively (Dalrymple et al., 1992; Dalrymple and Choi, 2007). The large- and small-scale cross-stratification in this facies corresponds to bar deposits in the subtidal and intertidal zones, respectively (Clifton, 1983; Dalrymple et al., 1990). The multiple erosive surfaces in this facies reflect the complex tidal channel networks (Hughes, 2012). The presence of tidal influence is also implied by the mud drapes in this facies (Visser, 1980; Tessier and Gigot, 1989). In particular, double mud drapes indicate tidal-slack water deposition (Fenies et al., 1999; Mackay and Dalrymple, 2011). The conglomerate underlying this facies is interpreted as a tidal ravinement surface formed by erosion with strong tidal currents during transgression (Cattaneo and Steel, 2003).

3.3.2 Facies 7: tidal flat

Description. Facies 7 consists of medium-grained sandstone characterized by bioturbation of *Schaubcylindrichnus* isp., which is identified by a convex downward tube of ~2 cm in diameter (Fig.7F). This facies is intercalated in the sandstones of Facies 6. Parallel stratification is observed with horizontal mud drapes (~1 cm thick) that laterally disappear within a few meters. Small-scale cross-stratification (10–20 cm in set height) can also be observed (Figs.6A and 8D).

Interpretation. Facies 7 is interpreted as tidal flat deposits. Tidal flats are flat-shaped geomorphology in an intertidal zone, often bioturbated and parallel-stratified (Desjardins et al., 2012). *Schaubcylindrichnus* isp. is a crustacean burrow frequently observed in tidal flat deposits (Nara, 2006).

3.3.3 Depositional Environment of Facies Association III

Facies Association III is a succession of tide-dominated estuary deposits, consisting of tidal sand bar (Facies 6) and tidal flat (Facies 7) deposits (Fig.6C). This facies association is characterized by large-scale cross stratification significantly influenced by tides, and it overlies Facies Association II, bounded by the tidal ravinement surface (Fig.3).

Tidal flat deposits (Facies 7) often appear at the top of tidal sand bar (Facies 6) deposits (Figs.6A and 8B). In a vertical tidal sand bar succession, the sand bar deposits can be capped by tidal flat deposits that are bioturbated and parallel- or cross-stratified (Dalrymple et al., 1990). Considering a set composed of Facies 6 and 7, the units of the sand bar and tidal flat deposits are ~10–15 m in thickness (Figs.6A and 8B). The mud drapes in Facies 7 are more abundant than those in Facies 6, probably reflecting the vertical decrease in tidal current speeds (Dalrymple and Choi, 2007).

The tidal sand bar deposits can be compared with those in modern estuaries. Leuven et al. (2016) compiled bar heights from modern tide-dominated estuaries and reported a range of approximately 3–20 m. The bar thickness of approximately 10–15 m observed in the Urahoro Group is comparable to that of the Mersey Estuary (UK) and the Coosaw River Estuary (USA). Additionally, using the relationship between bar height, bar length, and estuary depth proposed by Leuven et al. (2016), the bar height in the Urahoro Group suggests that Facies 6 extends several kilometers, with an estimated paleo-depth of approximately 10–15 m.

The tidal influence of this facies association is conformable to the sediment provenance analysis of the Urahoro Group. Throughout the depositional periods of the three formations examined in this study, the sediment provenance was consistently located west, based on the gravel compositions. Previous studies estimated the sediment provenance of the Group to be from the Upper Cretaceous to Paleogene Nikoro Group located in the westward of the Shiranuka-hill region (Sato et al., 1967; Nanayama et al., 1994) (Fig.1B). The U-Pb age distributions of the detrital zircons in the Urahoro Group also suggest that there was no sediment provenance transition during the deposition of the Group. However, Sato et al. (1967) suggested that the northwestward paleocurrent in the Shitakara Formation implies an uplift of a landmass in the southeast area of the depositional basin. This study revealed that the paleocurrents showing multiple directions occur in the tidal sand bar deposits (Facies 7) of the Shitakara Formation (Fig.6A). Thus, the northwestward paleocurrent can be interpreted as the influence of tides in the estuarine environment.

4 Discussion

4.1 Transgression in the Urahoro Group

The transgression in the Urahoro Group from alluvial fan to estuarine environments can be attributed to the tectonic subsidence of the basin. Nanayama et al. (1994) speculated that the transgression in the Urahoro Group was owed to the eustatic sea-level change, while the depositional age of the Group was uncertain at that time. Recently, several studies have indicated that the Urahoro Group was deposited from 39 Ma (the Harutori Formation) to 36 Ma (the Shakubetsu Formation) based on the U-Pb ages of zircon grains (Katagiri et al., 2020; Harisma et al., 2024; Takeshita et al., 2025). The amplitude of the eustatic sea-level change was estimated to be approximately 50 m during this period (Miller et al., 2020). In contrast, the transgressive succession in the Urahoro Group was >300 m thick, and the paleo-bathymetry estimated from the facies increased during the deposition of the succession. Thus, relative sea level increased by several hundred meters in the sedimentary basin of the Urahoro Group during deposition, which is difficult to explain by the eustatic sea-level change.

The subsidence rate experienced by the Urahoro Group is considerably faster than that of typical sedimentary basins. Sinclair and Naylor (2012) reviewed the subsidence rates of various foreland basins and reported typical values of around 50 m/Myr. For smaller forearc basins, Sakai and Masuda (1998) documented that the tectonic subsidence rate of the rapidly subsiding Kakegawa Group ranged from approximately 100 to 200 m/Myr. Compared to these documented rates, the Urahoro Group, experiencing subsidence exceeding 300 m within a span of 1–3 Myr, can be regarded as having undergone remarkably rapid subsidence.Katagiri et al. (2020) estimated the collision of the Paleo-Kuril Arc and the

Northeastern Japan Arc was progressing around 40 Ma, and the tectonic bending of the region occurred due to the oblique arc-arc collisional process during the depositional period of the Urahoro Group. This tectonic event may have been related to the exceptionally rapid subsidence of the basin.

4.2 Transition of Dominant Process in Estuarine Environment

This study illustrated the developmental path from wave-dominated to tide-dominated estuaries in the Urahoro Group, which differs from the conventional development model proposed in previous studies. Several evolutionary models of wave-dominated estuary, where systems develop into deltas or remain in wave-dominated morphology, are described in the Introduction (Roy et al., 1980; Dalrymple et al., 1992; Anthony et al., 2002; Harris and Heap, 2003).

Although no previous estuarine study has reported cases from wave- to tide-dominated morphological change, there are two examples of the Holocene estuarine depositional records that allogenically transitioned from tide- to wave-dominated environments, implying the significance of external controls of estuarine environments. Pendón et al. (1998) reported the morphological transition of the Holocene Domingo-Rubio estuarine system in southwestern Spain. The Domingo-Rubio Estuary is located in the outlet region of the two adjacent wider estuaries and is initially dominated by tidal depositions. The adjacent estuaries subsequently developed tidal sand bars lying perpendicularly at the mouth of the Domingo-Rubio estuary. The sand bars played a role as a barrier island for the Domingo-Rubio estuary, which consequently turned into a wave-dominated estuary as fine-grained sediments were deposited in its central part. Williams et al. (2013) also described the geomorphic shift of the Holocene Nakdong Estuary in southeastern South Korea. The mi- crotidal Nakdong Estuary was initially tide-dominated with a funnel-shaped geometry and limited mouth barrier construction. A series of anthropogenic alterations (constructions of dams and reclamations) from 1980 modified estuarine geometry and decreased tidal activ- ity. The alterations eventually resulted in the development of several mouth bars, which characterize the wave-dominated estuary. These examples suggest that external factors may cause a transition in dominant environmental controls and modify fundamental estuarine geomorphologies.

Here, we propose a possible hypothesis to explain the exceptional transition from wave- to tide-dominated estuary observed in this study (Fig.9). A possible external cause of the estuarine environmental transition in the Urahoro Group is a rapid relative sea-level rise. The mouth barrier that characterizes the wave-dominated estuary can be disintegrated due to an accelerated rate of relative sea-level rise. A conceptual model with natural examples illustrates the response of barriers to sea-level rise (FitzGerald et al., 2008, 2018). According to this model, a rapid sea-level rise increases the tidal prism and water discharge through tidal inlets, which erode and enlarge them. While the increasing tidal prism contributes to the growth of ebb- and flood-tidal deltas, the enlarged tidal inlet/basin system intensifies flood dominance in the tidal regime (Van Goor et al., 2003; Dissanayake et al., 2012). Flood dominance facilitates a substantial landward influx of sandy sediments, leading to extensive back-barrier sand bodies at the expense of sandy sediments comprising the barrier (FitzGerald and Montello, 1993) (9B). The barrier disintegration in the Urahoro Group is indicated by the flood-tidal delta deposits (Facies 5) of Facies Association II.

Although the developmental process involving such morphological transitions in estuaries has not been thoroughly documented, similar examples might be identified in other tectonically active settings in the future. The Urahoro Group is estimated to have been deposited during an arc-arc collision event (Kimura and Kusunoki, 1997; Katagiri et al., 2016, 2020). A large-scale tectonic event in the arc-arc collision may have increased the subsidence rate in the depositional basin of the Urahoro Group, contributing to the observed changes. To better understand the impacts of potential rapid global sea-level changes on coastal geomorphology, integrated research combining experimental studies, numerical modeling, and investigations of ancient examples is highly desirable for elucidating the controlling factors governing estuary morphotypes.

5 CONCLUSIONS

The depositional history of the Eocene Urahoro Group, from initial alluvial fan deposits to wave-dominated and subsequently tide-dominated estuarine environments, was reconstructed through detailed facies analysis. As the Urahoro Group in the Konsen coastal region is exposed along large-scale coastal cliffs that researchers cannot reach, the sedimentary deposits were investigated using a drone to take outcrop photographs and construct a 3D outcrop model in addition to a naked-eye field survey. This study focused on the Tenneru, Yubetsu, and Shitakara Formations, identifying seven fluvial to shallow marine facies grouped into three facies associations. The findings indicate that the wave-dominated estuary transitioned into a tide-dominated system within a transgressive succession. This study hypothesized that the transition may have been triggered by mouth-barrier disintegration of the wave-dominated estuary due to a rapid relative sea-level rise in the basin. Although previous development models of estuaries have suggested that the fundamental geomorphologies of estuaries are maintained throughout their depositional history, the present paper provides a new perspective of estuarine evolution from wave- to tide-dominance. Understanding the morphodynamics of estuaries contributes to the prediction of future morphological modifications in response to environmental changes.

ACKNOWLEDGEMENTS

The authors appreciate the Sediment Dynamics Research Consortium and the Fukada Geological Survey for funding this study. We thank INPEX Corporation for permitting the use of the three-dimensional model of the Urahoro Group's outcrop for this research.

REFERENCES CITED

Allen, G.P., 1971, Relationship between grain size parameter distribution and current patterns in the Gironde estuary (France). Journal of Sedimentary Research 41, 74–88.

Allen, G.P. and Posamentier, H.W., 1993, Sequence stratigraphy and facies model of an incised valley fill; the Gironde Estuary, France. Journal of Sedimentary Research 63, 378–391.

Allen, J.R.L., 1983, Studies in fluviatile sedimentation: bars, bar-complexes and sandstone sheets (low-sinuosity braided streams) in the Brownstones (L. Devonian), Welsh Borders. Sedimentary Geology 33, 237–293.

Anthony, E.J., Oyédé, L.M., and Lang, J., 2002, Sedimentation in a fluvially infilling, barrier-bound estuary on a wave-dominated, microtidal coast: the Ouémé River estuary, Benin, west Africa. Sedimentology 49, 1095–1112.

Aschoff, J.L., Olari, C., and Steel, R.J., 2018, Recognition and significance of bayhead delta deposits in the rock record: A comparison of modern and ancient systems. Sedimentology 65, 62–95.

Boyd, R., Dalrymple, R.W., and Zaitlin, B.A., 2006, Estuarine and incised-valley facies models. In: Posamentier, H.W. and Walker, R.G. (Eds.), Facies Models Revisited. SEPM Special Publications 84, pp. 171–234.

Bridge, J.S., 2003, Rivers and Floodplains: Forms, Processes, and Sedimentary Record. Blackwell Publishing, Oxford.

Bridge, J.S., 2006, Fluvial facies models: recent developments. In: Posamentier, H.W. and Walker, R.G. (Eds.), Facies Models Revisited. SEPM Special Publications 84, pp.

85–170.

Bridge, J.S. and Lunt, I.A., 2006, Depositional models of braided rivers. Blackwell Publishing, Oxford.

Cattaneo, A. and Steel, R.J., 2003, Transgressive deposits: a review of their variability. Earth-Science Reviews 62, 187–228.

Chaumillon, E., Tessier, B., and Reynaud, J.Y., 2010, Stratigraphic records and variability of incised valleys and estuaries along French coasts. Bulletin de la Société Géologique de France 181, 75-85.

Clifton, H.E., 1983, Discrimination between subtidal and intertidal facies in Pleistocene deposits, Willapa Bay, Washington. Journal of Sedimentary Research 53, 353-369.

Cooper, J.A.G., 1993, Sedimentation in a river dominated estuary. Sedimentology 40, 979–1017.

Dalrymple, R.W. and Choi, K., 2007, Morphologic and facies trends through the fluvial-marine transition in tide-dominated depositional systems: A schematic framework for environmental and sequence-stratigraphic interpretation. Earth-Science Reviews 81, 135-174.

Dalrymple, R.W., Knight, R.J., Zaitlin, B.A., and Middleton, G.V., 1990, Dynamics and facies model of a macrotidal sand-bar complex, Cobequid Bay-Salmon River Estuary (Bay of Fundy). Sedimentology 37, 577–612.

Dalrymple, R.W., Zaitlin, B.A., and Boyd, R., 1992, Estuarine facies models; conceptual basis and stratigraphic implications. Journal of Sedimentary Research 62, 1130- 1146.

Desjardins, P.R., Buatois, L.A., and Mangano, M.G., 2012, Tidal flats and subtidal sand bodies. Developments in Sedimentology 64, 529–561.

Dissanayake, D., Ranasinghe, R., and Roelvink, J., 2012, The morphological response of large tidal inlet/basin systems to relative sea level rise. Climatic change 113, 253–276.

de Fátima Rossetti, D., 2000, Influence of low amplitude/high frequency relative sea-level changes in a wave-dominated estuary (Miocene), São Luis Basin, northern Brazil. Sedimentary Geology 133, 295–324.

Fenies, H., Resseguier, A.D., and Tastet, J.P., 1999, Intertidal clay-drape couplets (Gironde estuary, France). Sedimentology 46, 1–15.

FitzGerald, D.M. and Montello, T.M., 1993, Backbarrier and inlet sediment response to the breaching of Nauset Spit and formation of New Inlet, Cape Cod, Massachusetts. In: Aubrey, D.G., and Giese, G.S. (Eds.), Formation and evolution of multiple tidal inlets 44. American Geophysical Institution, Washington, DC, pp. 158–185.

FitzGerald, D.M., Fenster, M.S., Argow, B.A., and Buynevich, I.V., 2008, Coastal impacts due to sea-level rise. Annual Review of Earth and Planetary Sciences 36, 601–647.

FitzGerald, D.M., Hein, C.J., Hughes, Z., Kulp, M., Georgiou, I., and Miner, M., 2018, Runaway barrier island transgression concept: Global case studies. In: Moore, L.J. and Brad Murray, A. (Eds.), Barrier dynamics and response to changing climate. Springer Nature, pp. 3–56.

Geological Survey of Japan, National Institute of Advanced Industrial and Science Technology, 2023, Seamless digital geological map of Japan V2 (original edition).

Geological Survey of Japan, National Institute of Advanced Industrial and Science Technology, Tsukuba, Japan.

Harisma, H., Niki, S., Hirata, T., and Naruse, H., 2024, Cretaceous to early Paleogene sediment provenance transition from continental to magmatic arc systems in the Northwestern Pacific Region. Scientific Reports 14, 7280. https://doi.org/10.1038/s41598-024-55471-1.

Harris, P.T. and Heap, A.D., 2003, Environmental management of clastic coastal depositional environments: inferences from an Australian geomorphic database. Ocean & coastal management 46, 457–478.

Hayes, M.O. and FitzGerald, D.M., 2013, Origin, evolution, and classification of tidal inlets. Journal of Coastal Research 69, 14–33.

Hughes, Z.J., 2012, Tidal channels on tidal flats and marshes. In: Davis Jr., R.A. and Dalrymple, R.W.(Eds.), Principles of tidal sedimentology. Springer, pp. 269–300.

Katagiri, T., Naruse, H., Hirata, T., and Hattori, K., 2016, U–Pb age of the tuff bed in the Urahoro Group, eastern Hokkaido, northern Japan. Journal of the Geological Society of Japan 122, 495–503.

Katagiri, T., Naruse, H., Ishikawa, N., and Hirata, T., 2020, Collisional bending of the western Paleo-Kuril Arc deduced from paleomagnetic analysis and U-Pb age determination. Island Arc 29, e12329. https://doi.org/10.1111/iar.12329.

Kawai, M., 1956, Geological map of Konbumori prefecture, scale 1: 50,000 and its explanatory text. Geological Survey of Japan, Tsukuba, Japan.

Khojasteh, D., Glamore, W., Heimhuber, V., and Felder, S., 2021, Sea level rise impacts on estuarine dynamics: A review. Science of The Total Environment 780, 146470. https://doi.org/10.1016/j.scitotenv.2021.146470.

Kimura, G. and Kusunoki, K., 1997, The Hidaka Orogeny and tectonics of arc-arc junction. Memory of Geological Society of Japan 47, 295–305.

Kumbier, K., Carvalho, R.C., and Woodroffe, C.D., 2018, Modelling hydrodynamic impacts of sea-level rise on wave-dominated Australian estuaries with differing geomorphology. Journal of Marine Science and Engineering 6, 66. https://doi.org/10.3390/jmse6020066.

Leuven, J., Kleinhans, M., Weisscher, S., and Van der Vegt, M., 2016, Tidal sand bar dimensions and shapes in estuaries. Earth-science reviews 161, 204–223.

Lorenzo-Trueba, J. and Ashton, A.D., 2014, Rollover, drowning, and discontinuous retreat: Distinct modes of barrier response to sea-level rise arising from a simple morphodynamic model. Journal of Geophysical Research: Earth Surface 119, 779–801.

Mackay, D.A. and Dalrymple, R.W., 2011, Dynamic mud deposition in a tidal environment: the record of fluid-mud deposition in the Cretaceous Bluesky Formation, Alberta, Canada. Journal of Sedimentary Research 81, 901–920.

Masselink, G. and van Heteren, S., 2014, Response of wave-dominated and mixed-energy barriers to storms. Marine Geology 352, 321–347.

Matsui, M., 1962, Sedimentological study of the Paleogene basin of Kushiro in Hokkaido, Japan. Journal of the Faculty of Science, Hokkaido University. Series 4, Geology and Mineralogy 11, 431–480.

Meijer, T. and Preece, R., 2000, A review of the occurrence of Corbicula in the Pleistocene of North-West Europe. Netherlands Journal of Geosciences 79, 241–255.

Miall, A.D., 2010, Alluvial deposits. In: James, N.P. and Dalrymple, R.W. (Eds.), Facies Models 4. Geological Association of Canada, pp. 105–137.

Miall, A.D., 1981, Analysis of fluvial depositional systems. American Association of Petroleum Geologists; Education Course Note Series 20.

Miller, K.G., Browning, J.V., Schmelz, W.J., Kopp, R.E., Mountain, G.S., and Wright, J.D., 2020, Cenozoic sea-level and cryospheric evolution from deep-sea geochemical and continental margin records. Science advances 6, eaaz1346. 10.1126/sciadv.aaz1346.

Moore, L. J., List, J. H., Williams, S. J., and Stolper, D., 2010, Complexities in barrier island response to sea level rise: Insights from numerical model experiments, North Carolina Outer Banks. Journal of Geophysical Research: Earth Surface 115, F03004. https://doi.org/10.1029/2009JF00129.

Nagahama, H., 1961, Geological map of Kushiro prefecture, scale 1: 50,000 and its explanatory text. Hokkaido Development Agency, Hokkaido, Japan.

Nanayama, F., Nakagawa, M., and Okada, H., 1994, Chemistry of detrital chromian spinels from the Eocene Urahoro Group, in the eastern Hokkaido and its origin. Journal of the Geological Society of Japan 100, 383–398.

Nara, M., 2006, Reappraisal of Schaubcylindrichnus: A probable dwelling/feeding structure of a solitary funnel feeder. Palaeogeography, Palaeoclimatology, Palaeoecology 240, 439–452.

Nichols, G. and Fisher, J., 2007, Processes, facies and architecture of fluvial distributary system deposits. Sedimentary geology 195, 75–90.

Nichols, M.M., Johnson, G.H., and Peebles, P.C., 1991, Modern sediments and facies model for a microtidal coastal plain estuary, the James Estuary, Virginia. Journal of Sedimentary Research 61, 883–899.

Nio, S.D., van den Berg, J.H., Goesten, M., and Smulders, F., 1980, Dynamics and sequential analysis of a mesotidal shoal and intershoal channel complex in the Eastern Scheldt (southwestern Netherlands). Sedimentary Geology 26, 263–279.

Ogg, J.G., 2012, Geomgnetic polarity time scale. In: Gradstein, F. M., J. G. Ogg, M. D. Schmiz, and G. M. Ogg (Eds.), The geologic time scale. Elsevier, pp. 85–113.

Pendon, J.G., Morales, J.A., Borrego, J., Jimenez, I., and Lopez, M., 1998, Evolution of estuarine facies in a tidal channel environment, SW Spain: evidence for a change from tide-to wave-domination. Marine Geology 147, 43–62.

Reineck, H.E. and Wunderlich, F., 1968, Classification and origin of flaser and lenticular bedding. Sedimentology 11, 99-104.

Richards, M.T., 1994, Transgression of an estuarine channel and tidal flat complex: the Lower Triassic of Barles, Alpes de Haute Provence, France. Sedimentology 41, 55–82.

Roy, P., Thom, B., and Wright, L., 1980, Holocene sequences on an embayed high-energy coast: an evolutionary model. Sedimentary Geology 26, 1–19.

Sakai, T. and Masuda, F., 1998, The relationship between glacio-eustatic parasequences and a third-order sequence in the Kakegawa Group, central Japan. Sedimentary geology 122, 95–107.

Sambrook Smith, G., Ashworth, P., Best, J., Woodward, J., and Simpson, C., Simpson, 2006, The sedimentology and alluvial architecture of the sandy braided South Saskatchewan River, Canada. Sedimentology 53, 413–434.

Sasa, Y., 1940a, Stratigraphy of the tertiary deposits in the Kushiro coal field and a critical review of the opinions expressed. Journal of Hokkaido Coal Mine Association 307, 1–19.

Sasa, Y., 1940b, Stratigraphy of the tertiary deposits in the Kushiro coal field and a critical review of the opinions expressed. Journal of Hokkaido Coal Mine Association 308, 1–24.

Sato, S., Sasa, Y., Hirokawa, O., Okazaki, Y., and Nagahama, H., 1967, The paleocurrent of the Paleogene in the East of Kushiro City. Journal of the Geological Society of Japan 73, 563–572.

Simms, A.R., Rodriguez, A.B., and Anderson, J.B., 2018, Bayhead deltas and shorelines: Insights from modern and ancient examples. Sedimentary Geology 374, 17–35.

Sinclair, H. and Naylor, M., 2012, Foreland basin subsidence driven by topographic growth versus plate subduction, Bulletin 124, 368–379.

Takeshita, T., Ito, H., and Kaji, H., 2025, Zircon U–Pb Dating of the Urahoro Group and Atsunai Formation in the Shiranuka Hills of Eastern Hokkaido, Northeast Japan: Implications for Tectonic Development. Island Arc 34, e70006. https://doi.org/10.1111/iar.70006.

Tanai, T., 1957, Geological map of Onbetsu prefecture, scale 1: 50,000 and its explanatory text. Hokkaido Development Agency, Hokkaido, Japan.

Tessier, B. and Gigot, P., 1989, A vertical record of different tidal cyclicities: an example from the Miocene Marine Molasse of Digne (Haute Provence, France). Sedimentology 36, 767–776.

Van Goor, M., Zitman, T., Wang, Z., and Stive, M., 2003, Impact of sea-level rise on the morphological equilibrium state of tidal inlets. Marine Geology 202, 211–227.

Visser, M., 1980, Neap-spring cycles reflected in Holocene subtidal large-scale bedform deposits: a preliminary note. Geology 8, 543–546.

Wells, H.W., 1961, The fauna of oyster beds, with special reference to the salinity factor. Ecological Monographs 31, 239–266.

Williams, J. R., Dellapenna, T. M., and Lee, G., 2013, Shifts in depositional environments as a natural response to anthropogenic alterations: Nakdong Estuary, South Korea. Marine Geology 343, 47–61.

Zhang, K., Douglas, B., and Leatherman, S., 2002, Do storms cause long-term beach erosion along the US East Barrier Coast? The Journal of Geology 110, 493–502.

FIGURE CAPTIONS

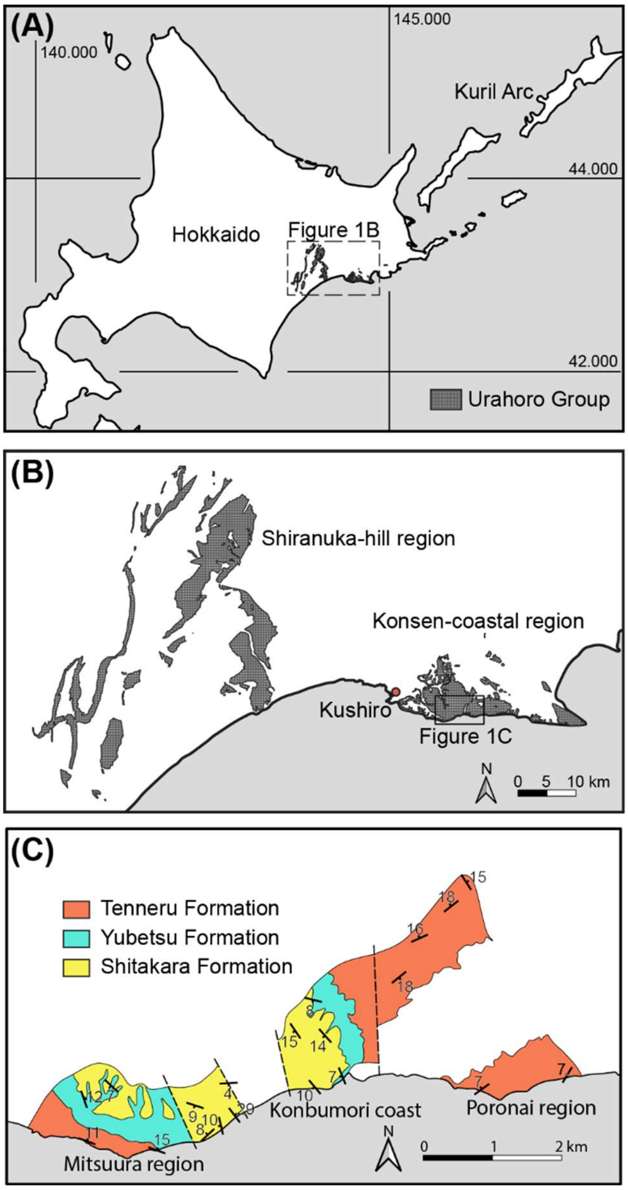

Fig. 1: Geological setting of the Urahoro Group. A. Location of the study area. The Urahoro Group is located in eastern Hokkaido, northern Japan. B. Distribution of the Urahoro Group. The Konsen Coastal Region is the target area of this study. The maps were modified after Geological Survey of Japan, National Institute of Advanced Industrial and Science Technology (2023). C. Geological map of the Urahoro Group distributed throughout the study area.

	Lithology		Fossils and Trace fossils	Depositional environment
1	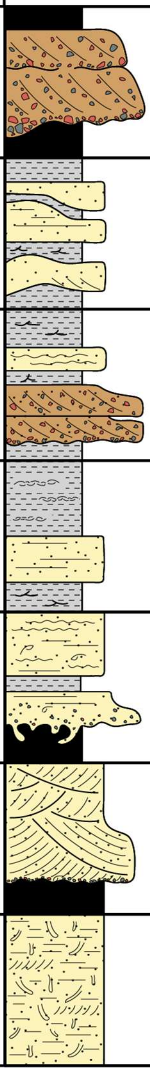	Gravely coarse sandstone -Poorly sorted -Cross-stratification -Grading -Erosional surface	Rootlet fossils	Braided river channel
2		Alternation of fine-grained sandstone and mudstone -Weakly laminated -Lateral thining	Rootlet fossils	Flood plain
3		Medium- to coarse-grained sandstone -Wave ripple -Including guranule to pebbles -Cross-stratification -Intercalated coaly mudstones	Rootlet fossils	Bayhead delta
4		Mudstone -Thin bedded fine sandstone Medium-grained sandstone -Parallel-stratification	Rootlet fossils *Corbicula* sp.	Central basin
5		Medium-grained muddy sandstone -Wavy-flaser ripple Medium to coarse-grained sandstone -Poorly sorted -Erosional surface	*Gyrolithes* isp. *Ostrea* sp. *Nemocardium* sp.	Flood-tidal delta
6		Medium-grained sandstone -Cross-stratification -Multiple directions of paleocurrent -Mud drapes	*Ostrea* sp.	Tidal sand bar
7		Medium-grained sandstone -Mud drapes -Cross-stratification	*Schaubcylindrichnus* isp.	Tidal flat

Fig. 2: Facies description and interpreted depositional environments of the Urahoro Group. The numbers on the left side of the columnar sections indicate the facies. See Fig.6A for legend.

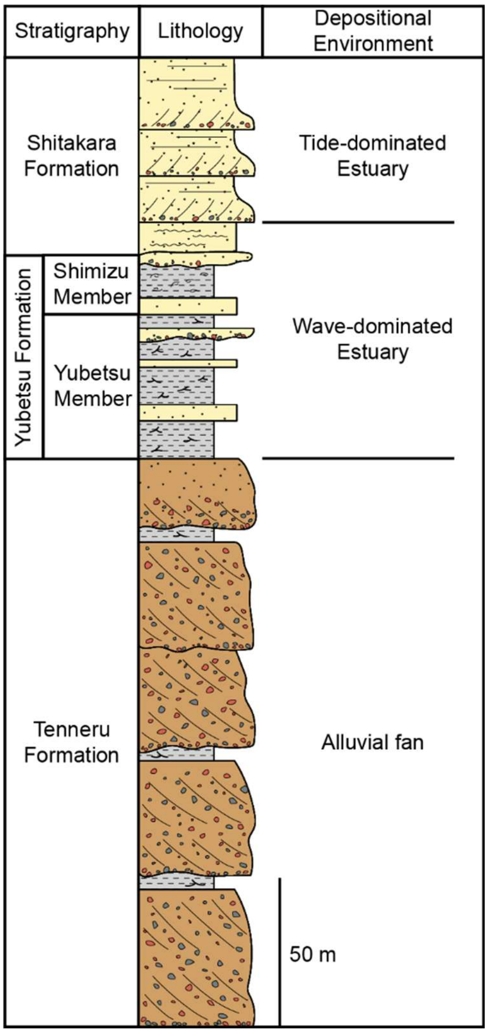

Fig. 3: Stratigraphy of the Urahoro Group distributed in the study area. The depositional environments are interpreted to be fluvial to shallow marine, as discussed in the text. See Fig.6A for legend.

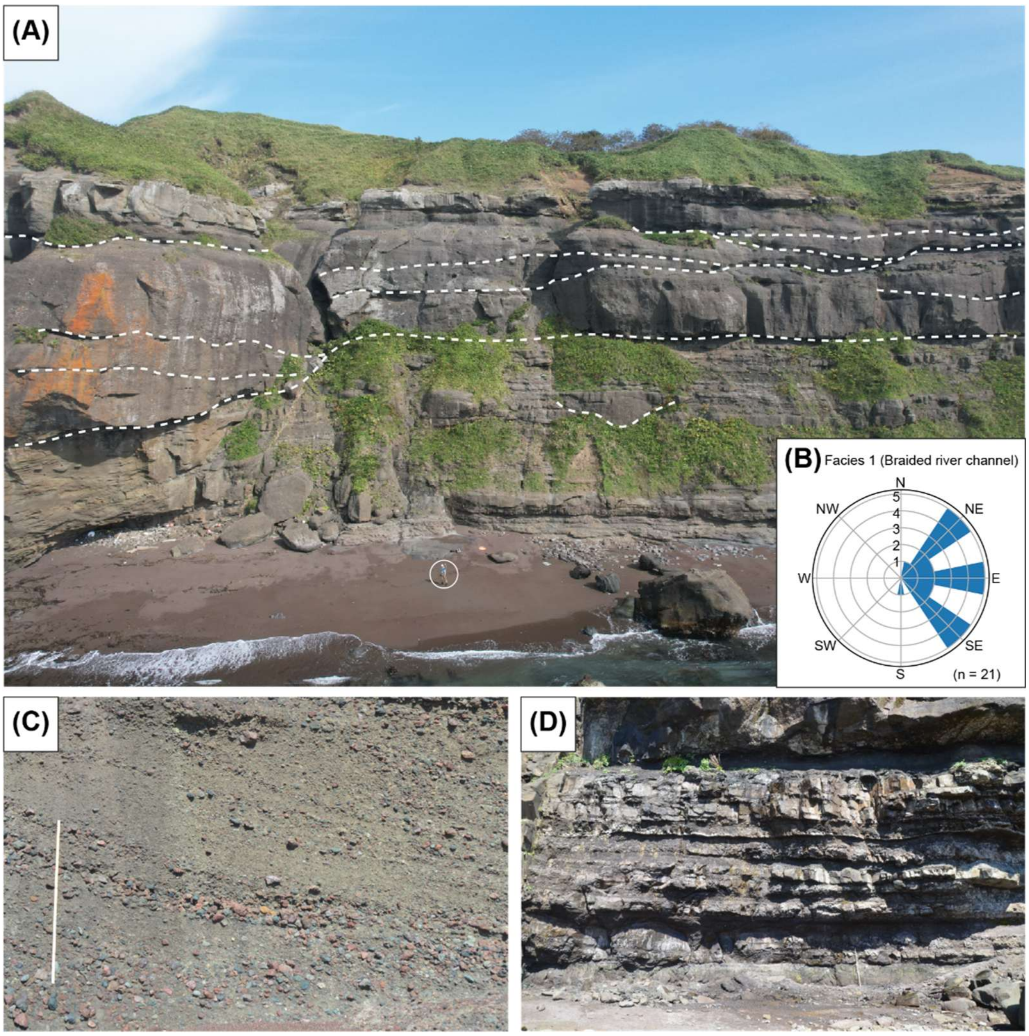

Fig. 4: Outcrop photographs of the deposits of Facies Association I (alluvial fan) of the Tenneru Formation in the Poronai region (Fig.1C). A. Outcrop exposing conglomerates (Facies 1) and alternation of sandstone and mudstone (Facies 2). The erosional bases in Facies 1 are indicated by the white dashed line. The white circle indicates a 1.8 meter human for scale. B. Paleocurrent directions acquired from Facies 1 distributed in the Mitsuura and Poronai regions (Fig.1C). C. Poorly sorted sandstones and clast-supported conglomerates in Facies 1 showing trough cross-stratification. The ruler is 1 m. D. Alternation of sandstone and mudstone (Facies 2) with unstable thickness. The ruler is 1 m long.

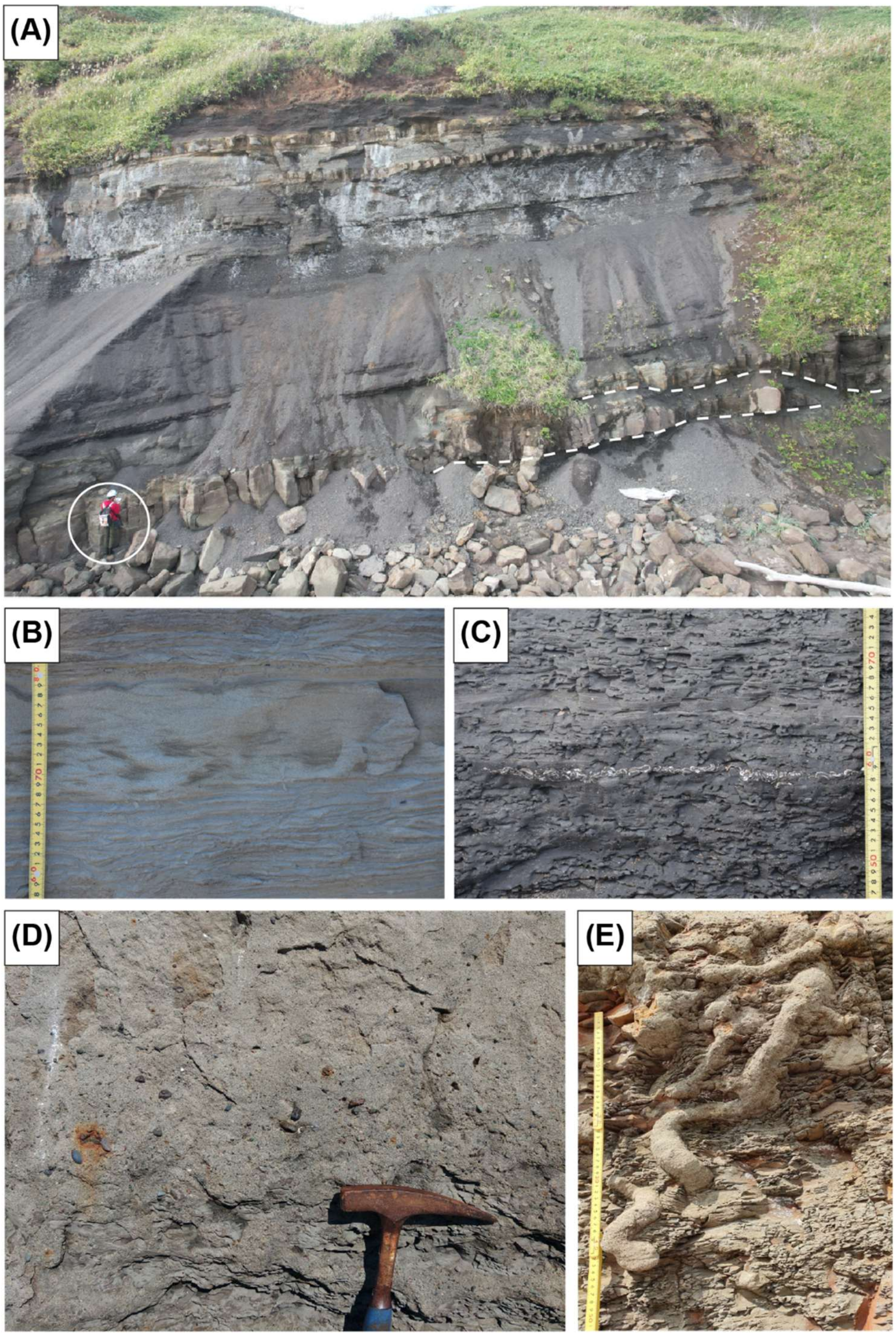
(A)
(B)
(C)
(D)
(E)

Fig. 5: Outcrop photographs of the deposits belonging to Facies Association II (wave-dominated estuary) of the Yubetsu Formation at the Konbumori coast (Fig. 1C). A. Outcrop exposing gravely sandstone and thickly bedded mudstone (Facies 3). The dashed lines indicate the erosional base of the gravelly sandstone. The parallel-laminated sandstone strata are located in the upper part of the outcrop at the boundary between Facies 3 and 4, above which sandy mudstones appear. This outcrop is a locality in the easternmost columnar section in Fig. 6A. The white circle indicates a 1.8-meter human scale. B. Fine-grained sandstone with wave ripples and mud drapes (Facies 3). C. Sandy mudstone displaying sand lenses and cumulative deposition of Corbicula sp. (Facies 4). D. Fining-upward gravelly sandstone of Facies 5 at the boundary with Facies 4. E. Bioturbation of *Gyrolithes* isp. of Facies 5 at the boundary with Facies 4. The borrows are characterized by spiral shapes protruding into the underlying mudstones.

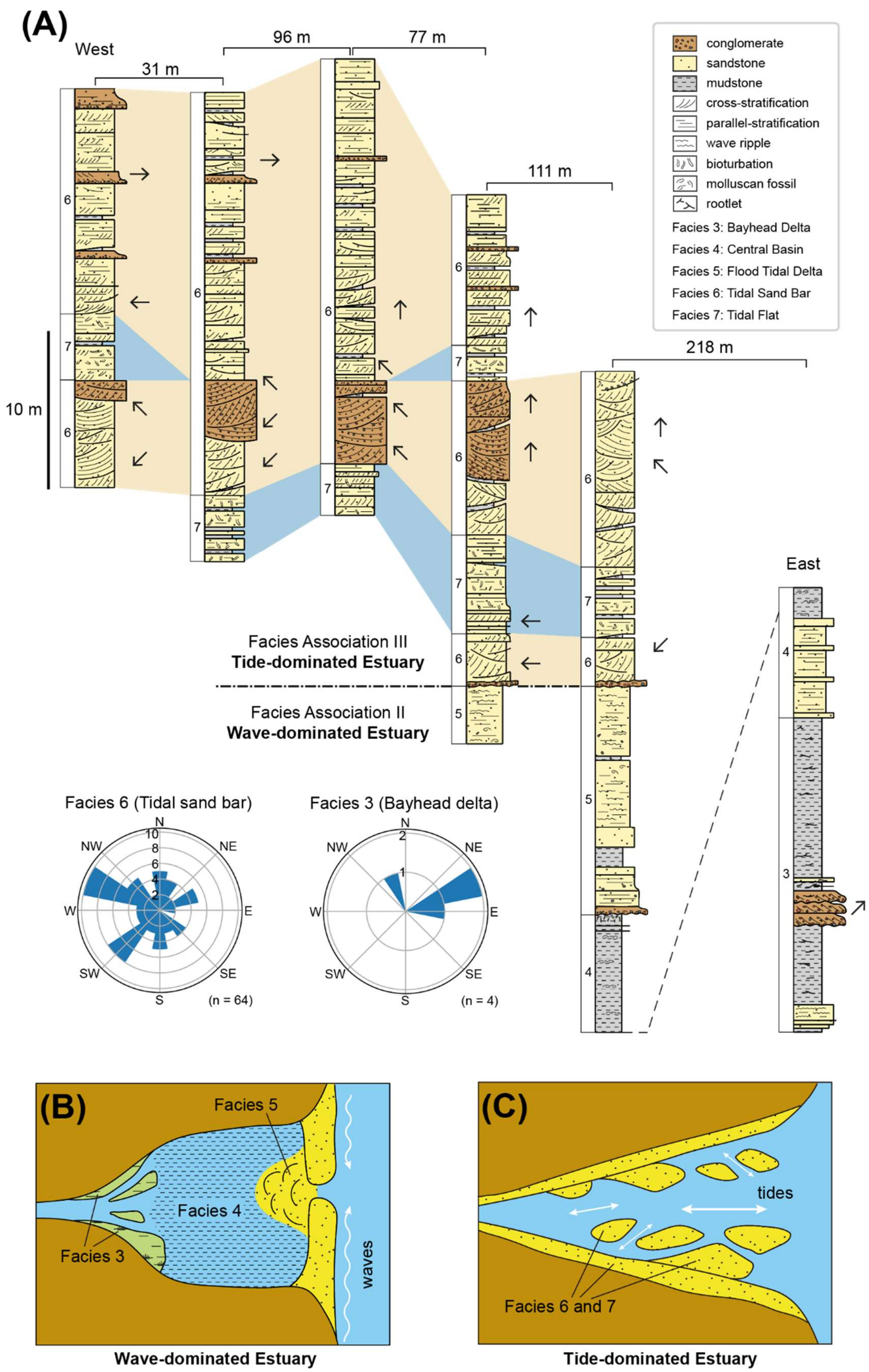
(A)
West
31 m
96 m
77 m
111 m
218 m
East
10 m
conglomerate
sandstone
mudstone
cross-stratification
parallel-stratification
wave ripple
bioturbation
molluscan fossil
rootlet
Facies 3: Bayhead Delta
Facies 4: Central Basin
Facies 5: Flood Tidal Delta
Facies 6: Tidal Sand Bar
Facies 7: Tidal Flat
Facies Association III
Tide-dominated Estuary
Facies Association II
Wave-dominated Estuary
Facies 6 (Tidal sand bar)
(n = 64)
Facies 3 (Bayhead delta)
(n = 4)
(B)
Facies 5
Facies 4
Facies 3
waves
Wave-dominated Estuary
(C)
tides
Facies 6 and 7
Tide-dominated Estuary

750

Fig. 6: Transition from wave- to tide-dominated estuary. A. Columnar sections of the Urahoro Group were acquired in the Konbumori coast based on the field observation (Fig. 5A) and a 3D outcrop model (Fig. 8A). The paleocurrent directions obtained from Facies 3 and 6 are shown in the rose diagrams based on the naked-eye observation in the field survey. The paleocurrent directions along the columnar sections are described based on the observation of the 3D outcrop model (Fig. 8A). B. Depositional environment of wave-dominated estuary (Facies Association II). This facies association consists of Facies 3–5 and is characterized by a mouth barrier formed by strong wave activity. C. Depositional environment of tide-dominated estuary (Facies Association III). This facies association consists of Facies 6 and 7 and is characterized by elongated sand bars reflecting strong tidal currents.

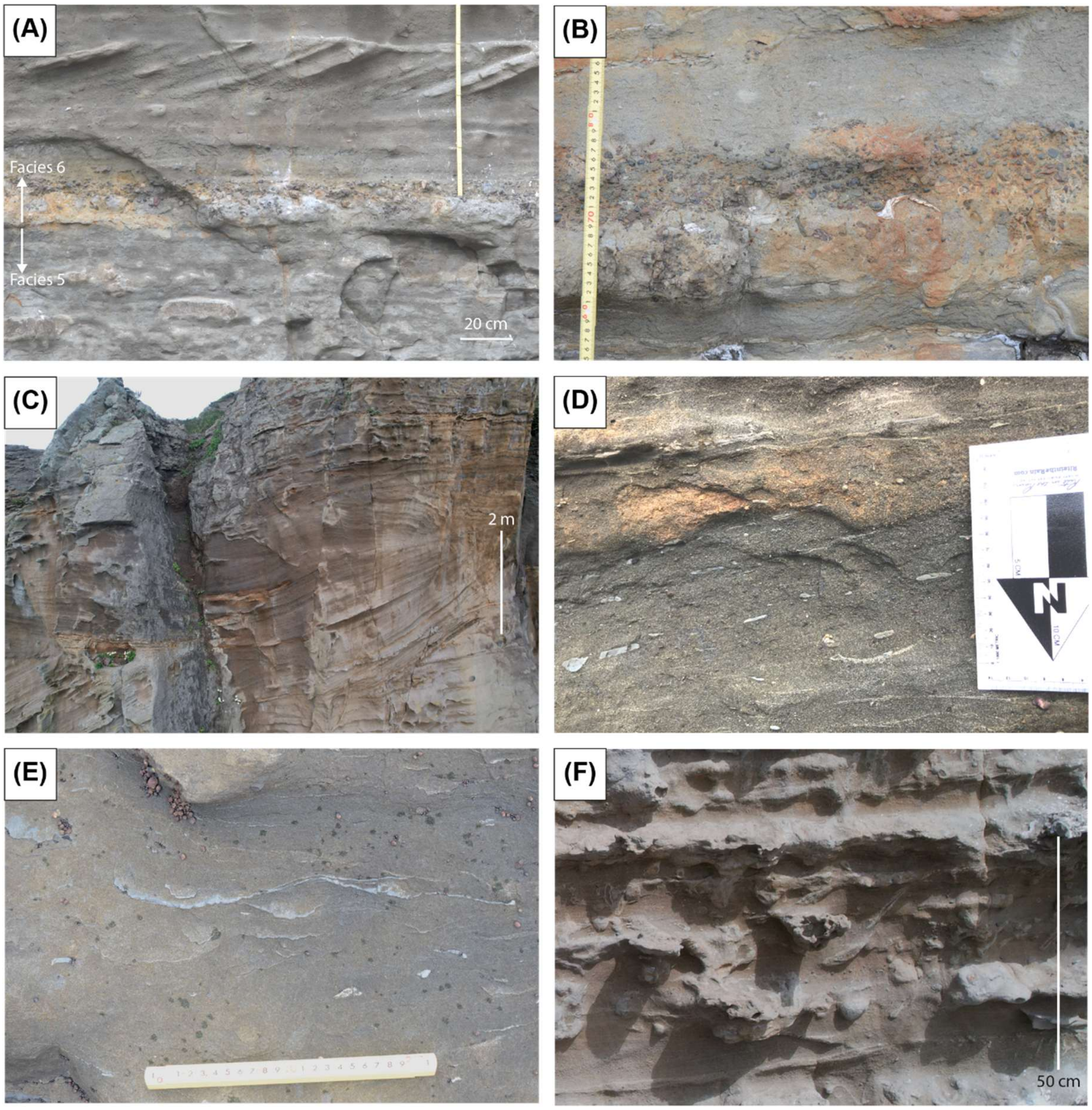
(A)
Facies 6
Facies 5
20 cm
(B)
(C)
2 m
(D)
(E)
(F)
50 cm

Fig. 7: Outcrop photographs of the deposits belonging to tide-dominated estuary facies association of the Shitakara Formation at the Konbumori coast (Fig. 1C). A. The boundary between Facies 5 and 6. The pebble conglomerate erodes the fine-grained sandstone exhibiting wavy-flaser ripple (Facies 5). B. Magnified photograph of the conglomerate in Fig. 7A. Well-sorted and rounded to surrounded pebbles and Ostrea sp. can be observed. C. Medium-grained sandstone displaying cross-stratification with a set height of ~2 m (Facies 6). D. Medium-grained sandstone displaying small-scale cross-stratification with mud drapes interbedded (Facies 6). E. Double mud drape observed in Facies 6. The ruler represents 20 cm. F. Schaubcylindrichnus isp. and parallel-stratification observed in Facies 7.

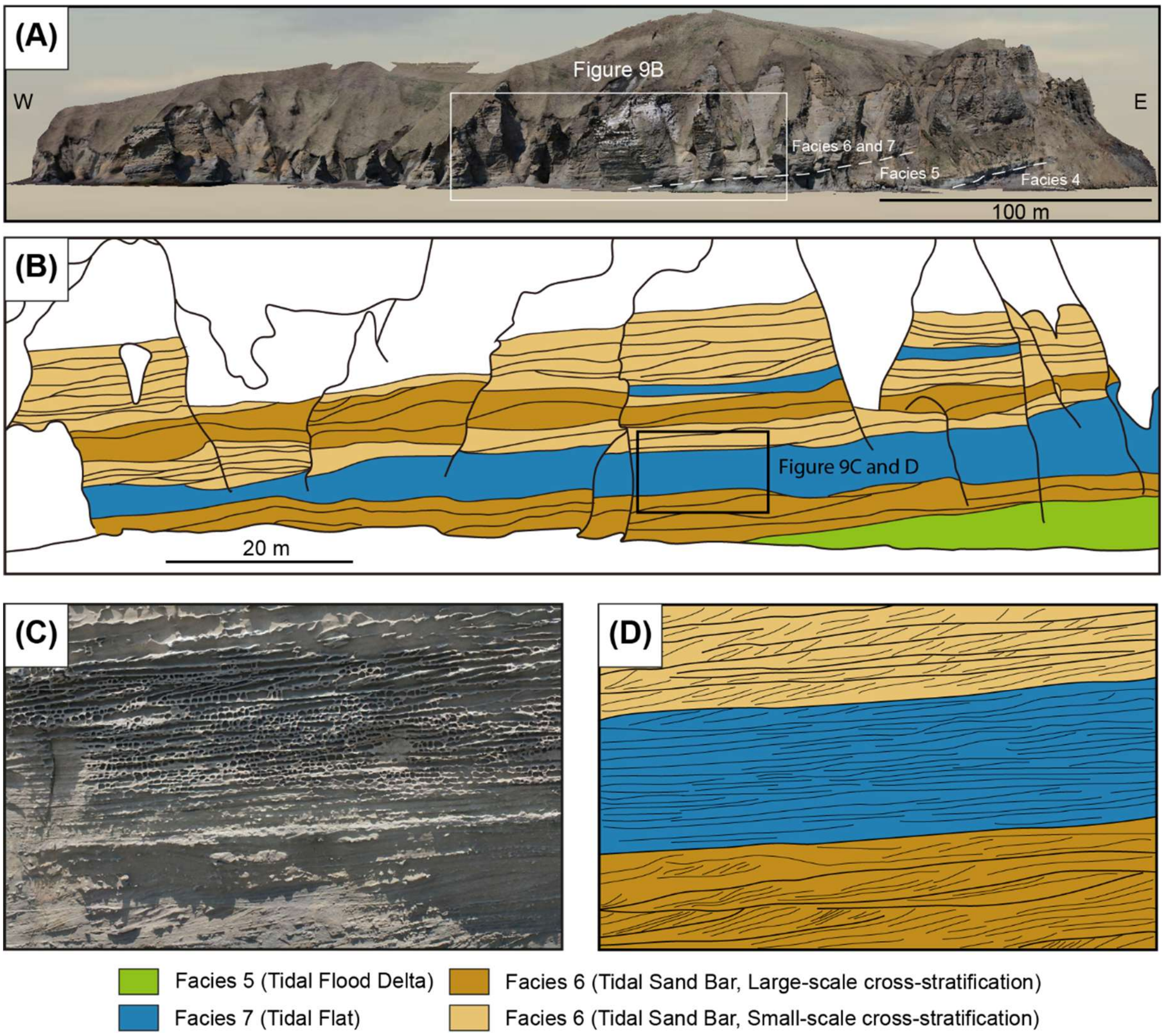

Fig. 8: Geological architectures observed in the Konbumori coast. A. 3D outcrop model constructed along the Konbumori coast, ranging 400 m width and ~50 m height. This outcrop is a locality for the five western columnar sections in Fig. 6A. B. Geological architectures of Facies 6 and 7 observed in the 3D outcrop model. The units of Facies 6 and 7 are ~10–15 m in thickness. C. Magnified photograph of the 3D outcrop model exhibiting Facies 6 and 7. D. The sedimentary structures observed in Facies 6 and 7 shown in Fig. 8C.

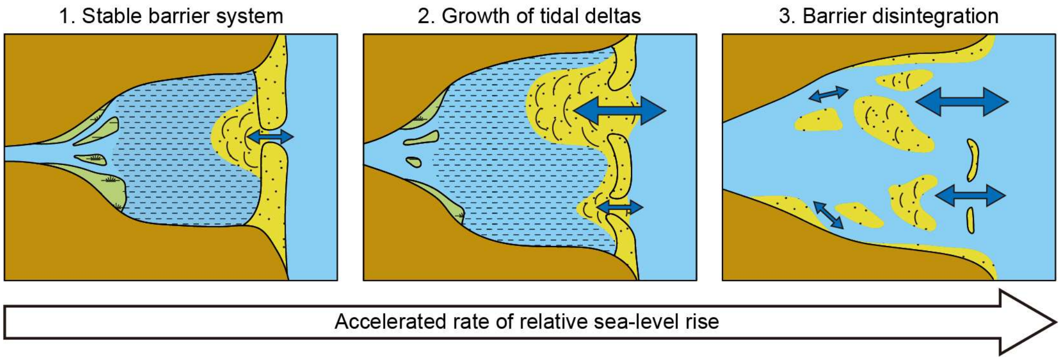

Fig. 9: Schematic of barrier disintegration. Due to the accelerated rate of relative sea-level rise, the increased tidal prism and flood-dominance at the tidal inlet expanded the back-barrier sand bodies, depleting the sandy sediments comprising the barrier. The bidirectional arrows indicate tidal currents.